



Cite this: *Dalton Trans.*, 2025, **54**, 1784

Received 14th November 2024,
Accepted 26th December 2024

DOI: 10.1039/d4dt03197k

rsc.li/dalton

Phenylphosphonic acid corroles: corroles that link and bind†

Gaëlle Divoux,‡ Margerite Loze,‡ Yoann Rousselin, Stéphane Brandès,
Claude P. Gros, * Nicolas Desbois * and Laurie André *

We report herein the synthesis and full spectroscopic characterization of two A₂B-corrole phosphonic acids. Thanks to the presence of a phosphonic acid functional group at the 10-*meso*-position, the corroles were covalently linked to the hexanuclear Zr clusters of a PCN-222 metal–organic framework (MOF). After the insertion of cobalt into the corrole macrocycle, the metal complexes are able to bind small volatile molecules such as carbon monoxide (CO). Interestingly, the resulting doped porous materials were used for selective detection of CO, with excellent selectivity for CO vs. CO₂, N₂, and O₂.

Introduction

Carboxylic and phosphonic acid functional groups have been widely used to anchor porphyrins onto the surface of organic and inorganic materials. While various substituted corroles bearing carboxylic groups, clickable functional groups or vinylic groups for further NIP and MIP polymerization have been widely described in the literature, only A₃-corroles bearing phosphonic acid groups have been reported so far.^{1,2} At the same time, many examples of surface modifications using organophosphonates and organophosphonic acids have appeared in various fields such as immobilization of catalysts and biological microarrays.^{3–5}

In this work, two A₂B-corroles functionalized with a phosphonic acid group at the *para*-position of the *meso*-10-phenyl substituent were synthesized (Scheme 1) and fully characterized. The difference between the two corroles lies in the electron withdrawing groups added at the 2,6-aryl positions, which

were expected to affect the Lewis acid character of the cobalt(III) centre^{6,7} and thus influence the efficiency of the CO binding to the corrole complex at low pressure. Indeed, we have previously reported that the affinity of cobalt corroles for CO depends on both the presence of a cobalt(III) ion and the Lewis acid character of the metal center.^{8–11}

Results

Synthesis of corroles 2a and 2b

5,15-(2,6-Dichlorophenyl)-10-diethylphenylphosphonic acid corrole (**1a**) and 5,15-(2,3,5,6-tetrafluorophenyl)-10-diethylphenylphosphonic acid corrole (**1b**) were prepared following the standard procedure described for the synthesis of A₂B-corroles using 0.5 equiv. of diethyl(4-formylphenyl)phosphonate and 1.0 equiv. of the corresponding dipyrromethane (ESI†). Hydrolysis of the diethylphosphonate groups was then performed using bromotrimethylsilane, leading to the target phosphonic acid corroles **2a–b** in almost quantitative yields with no further purification. The compounds were fully characterized by MALDI/TOF (low MS) and ESI (HRMS), UV-Vis and FTIR spectroscopy, and ¹H, ³¹P and ¹⁹F NMR spectroscopy.

An X-ray diffraction experiment was also carried out to fully confirm the structure of corrole **1b** (Fig. 1). Single clear dark violet, prism-shaped crystals of **1b** were isolated after recrystallization from a mixture of DCM and cyclohexane. Detailed information on the crystallographic data collection and refinement is given in the ESI.†

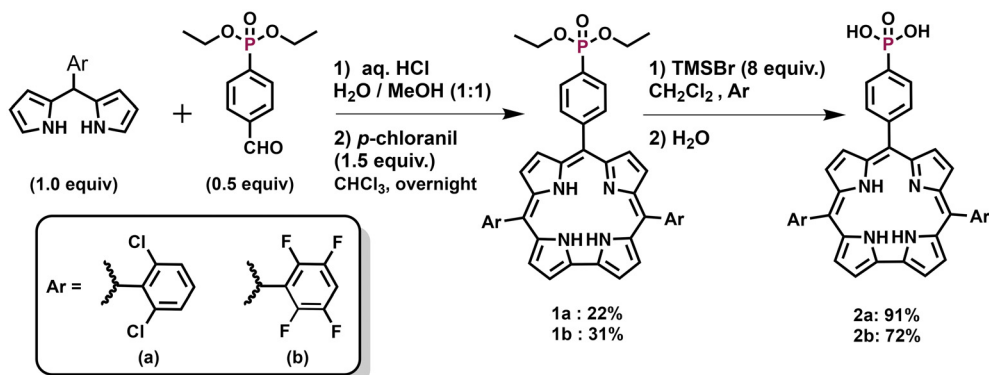
The arrangement of atoms in the solid form of compound **1b** (Fig. 1) is typical of –C₆F₄H-substituted corroles without a central metal atom. Three of the four pyrrole rings lie almost flat in a plane, while the remaining one bends out of the plane and forms a hydrogen bond with an oxygen atom from a nearby molecule. On average, the entire 23-atom ring system deviates by only 0.226 Å from a perfect plane, with the hydrogen-bonding pyrrole being the most out-of-plane at 0.424 Å. In Fig. 2, the crystalline packing is shown along the *a*-axis. The

Univ. Bourgogne Europe, CNRS, ICMUB (UMR 6302) Institut de Chimie Moléculaire de l'Université de Bourgogne, 9, Avenue Alain Savary, 21 000 Dijon, France.

E-mail: claud.gros@u-bourgogne.fr, nicolas.desbois@u-bourgogne.fr, laurie.andre@u-bourgogne.fr

† Electronic supplementary information (ESI) available. CCDC 2395038. For ESI and crystallographic data in CIF or other electronic format see DOI: <https://doi.org/10.1039/d4dt03197k>

‡ These authors contributed equally.



Scheme 1 Synthesis of phenylphosphonic acid corroles 2a and 2b.

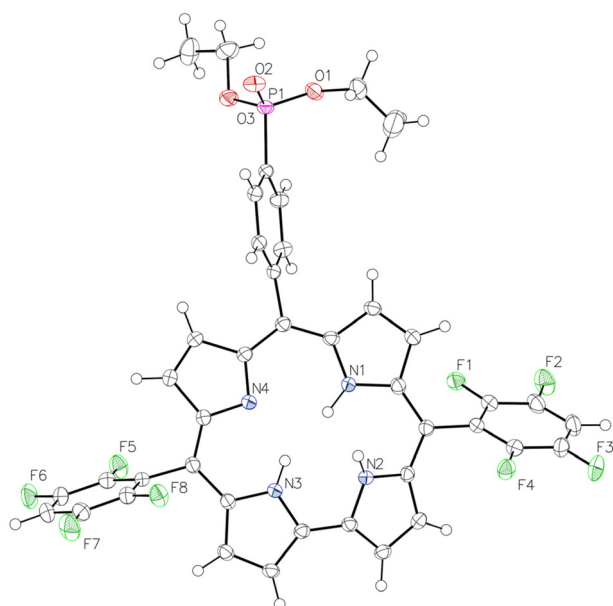


Fig. 1 ORTEP view of corrole 1b. Thermal ellipsoids are drawn at the 50% probability level. DCM solvent is omitted for clarity.

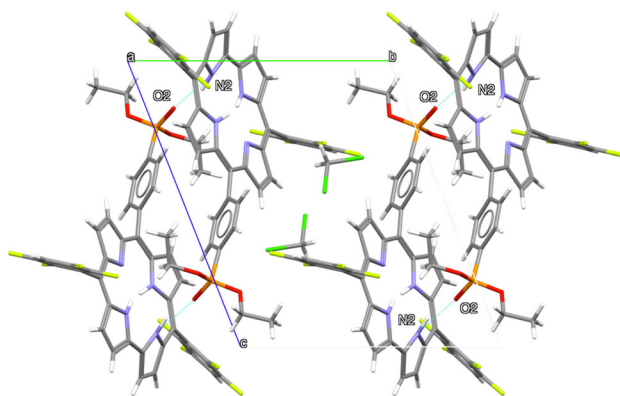


Fig. 2 View of the crystal packing of corrole 1b along a crystallographic axis. Intermolecular hydrogen bonds are depicted with blue dashed lines.

second molecule is generated *via* an inversion center (space group $P\bar{1}$). There is only one intermolecular hydrogen bond, connecting the oxygen atom O2 of the phosphonate group to the proton of the nitrogen atom N2 ($N2-H2\cdots O2 = 2.812(2)$ Å). This nitrogen atom N2 is distinctly oriented out of the porphyrin plane (-0.424 Å), as are the carbon atoms C8 (0.548 Å) and C9 (0.515 Å) of the same pyrrole group.

Synthesis of PCN-222

PCN-222 was synthesized through a modified solvothermal method similar to procedures reported in the literature.^{12,13} After the synthesis, PCN-222 was further activated by washing the MOF thoroughly with a solution of 0.1 M HCl/acetone in order to remove the modulator, dichloroacetic acid, present on the metal cluster. This activation releases the vacancies naturally present on the PCN-222 metal cluster and frees up space for further modification.

Synthesis of CoCorr(2a)@PCN-222 and CoCorr(2b)@PCN-222

The two studied corroles 2a and 2b were introduced into the activated PCN-222 by grafting on the free metal cluster vacancies of the MOF by reacting with the phosphonic acid functional groups. The grafting of the corroles 2a and 2b, respectively, produced the materials Corr(2a)@PCN-222 and Corr(2b)@PCN-222. The two obtained materials were then further metalated with cobalt (insertion of Co into the corrole macrocycles grafted inside the MOF) to obtain CoCorr(2a)@PCN-222 and CoCorr(2b)@PCN-222, respectively, for PCN-222 containing the cobalt complex of grafted corrole 2a and for PCN-222 containing the cobalt complex of grafted corrole 2b.

Characterization of CoCorr(2a)@PCN-222 and CoCorr(2b)@PCN-222 and structural stability

The corrole grafting ratio was calculated as the ratio of corrole present in the material to the porphyrin expected in the activated PCN-222, and it was determined using ¹H NMR by breaking down the materials using a solution of DCl and NaF in DMSO-*d*₆. The corrole grafting ratio was thus obtained as 0.2 corrole *per* porphyrin in CoCorr(2a)@PCN-222 and 0.39 in

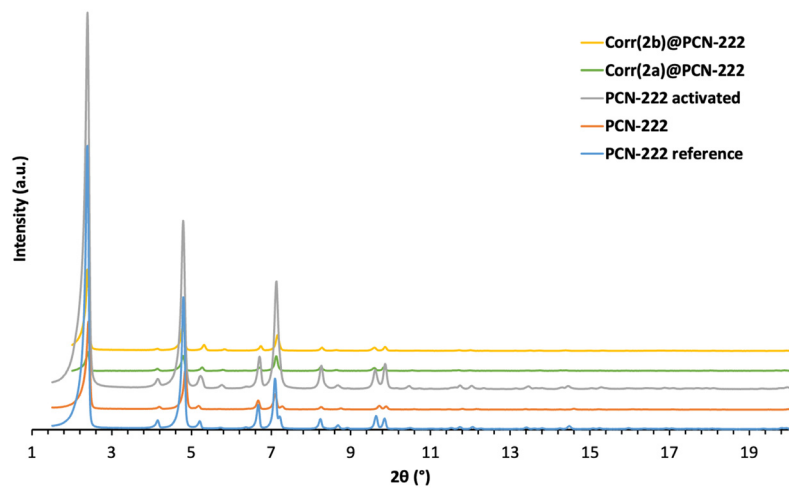


Fig. 3 Powder XRD analysis of the materials along the different modification steps.

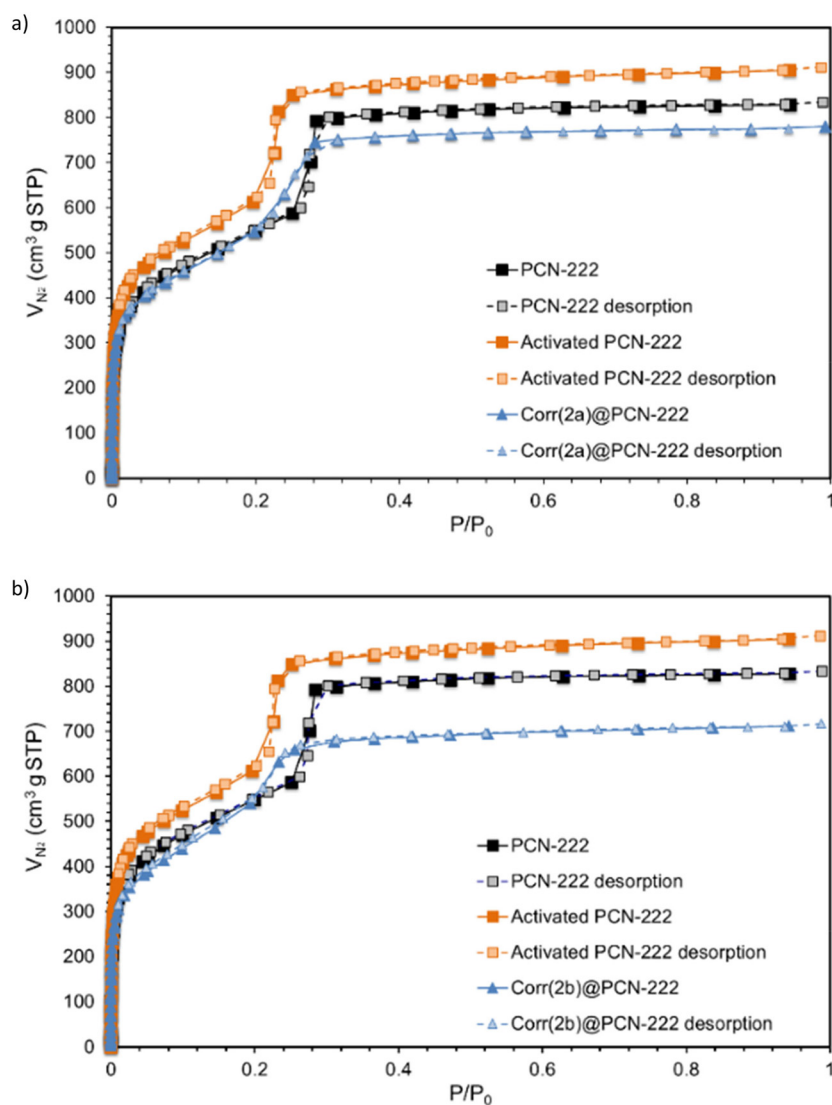


Fig. 4 N_2 adsorption isotherms recorded at 77 K for PCN-222, activated PCN-222 and grafted PCN-222 with corroles 2a and 2b.

CoCorr(2b)PCN-222. ICP measurements (Table S5†) reveal a metalation ratio of the grafted corroles of 80% for **CoCorr(2b)PCN-222**. For **CoCorr(2a)@PCN-222**, the cobalt ICP measurement is lower than expected, as systematically observed in all our samples with less than a certain quantity of corrole grafted (lower than 0.35).⁹ The structural stability of all the synthesized materials was studied using powder XRD (PXRD) (Fig. 3). All the materials present the same crystal structure, and the final materials **CoCorr(2a)@PCN-222** and **CoCorr(2b)PCN-222** maintain a stable and crystalline structure after undergoing the several modification steps required for their synthesis (Table S6†).

Porosity measurements

Further analysis of all the synthesized materials by BET measurements revealed the presence of both micropores and mesopores through a combination of typical adsorption type I and IV isotherms (Fig. 4). Specific surface areas of 1893.4 m² g⁻¹ and 1880.1 m² g⁻¹ were recorded for **Corr(2a)@PCN-222** and **Corr(2b)@PCN-222**, respectively. Both measurements are lower than those recorded for the as-synthesized PCN-222, 1947.6 m² g⁻¹, and for the activated PCN-222, 2143.0 m² g⁻¹, which is coherent with the successful grafting of corroles **2a** and **2b** inside PCN-222, resulting in less space in the MOF pores (Table 1).

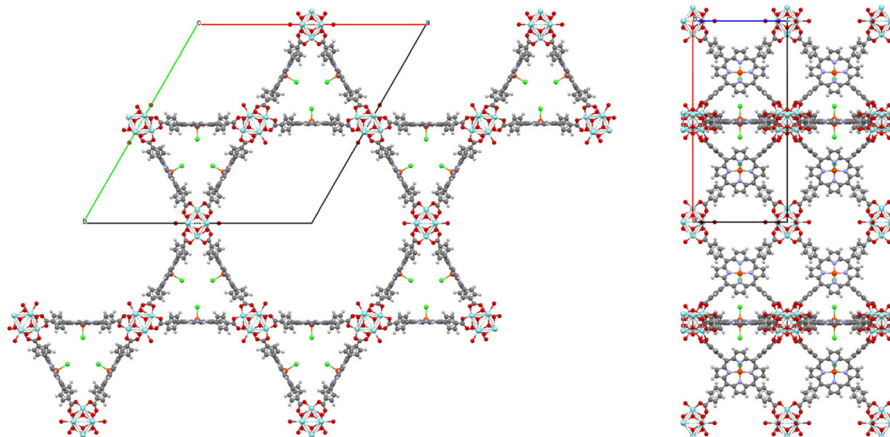
Carbon monoxide and carbon dioxide adsorption

Gas sorption measurements were conducted on **CoCorr(2a)@PCN-222** and **CoCorr(2b)@PCN-222**. The DMSO ligand resulting from the cobalt metalation step was first exchanged with more labile NH_{3(g)} ligands in order to allow the facile activation (removal of the axial ligands) of the cobalt corrole sites. Heating at 80 °C under vacuum removes the two

NH_{3(g)} molecules coordinated to the cobalt centers, making them readily available for further CO_(g) coordination. Then, the adsorption isotherms of CO_(g) vs. CO_{2(g)}, O_{2(g)} and N_{2(g)} were recorded (Fig. 5). For both samples, the steep slope corresponding to CO_(g) adsorption at low pressure is assigned to an efficient chemisorption process involving binding to the cobalt corrole. In parallel, a significant CO_{2(g)} intake through physisorption is noted, while N_{2(g)} and O_{2(g)} adsorbed volumes remain low, confirming the selectivity of the material for CO_(g), thanks to a chemisorption process. Indeed, the CO_(g) sorption shows a strong increase at very low pressure (<0.01 atm) that corresponds to selective sorption of CO_(g) on unsaturated sites of cobalt corroles. After saturation of the cobalt sites, physisorption dominates over chemisorption and this phenomenon results in a straight linear sorption process (Henry-type isotherm) for $P/P_0 > 0.02$. For **CoCorr(2a)@PCN-222**, at 1 atm, the CO_(g) volume adsorbed was 13.03 cm³ g⁻¹, while the CO_{2(g)} volume adsorbed was equal to 31.35 cm³ g⁻¹. **CoCorr(2b)@PCN-222** demonstrated better CO sorption, also due to a more efficient grafting of the corrole, and the volumes adsorbed at 1 atm were determined to be 15.93 cm³ g⁻¹ for CO_(g) and 30.50 cm³ g⁻¹ for CO_{2(g)}.

In order to describe more precisely the CO_(g) selectivity of our materials, the isotherms were fit with a double-site Langmuir model for CO_(g) adsorption and with a single-site Langmuir model for CO_{2(g)}, O_{2(g)} and N_{2(g)}. Fitting curves and fitting parameters are given in Fig. S25 and S26, and in Tables S7 and S8.† The selectivity of the two materials for CO_(g) over CO_{2(g)}, O_{2(g)} and N_{2(g)} was calculated using Henry's selectivity at 298 K at zero loading and is given in Table 2. These calculations confirm the relatively high selectivity of CO_(g) over CO_{2(g)}, O_{2(g)} and N_{2(g)}, particularly at low pressure, where selectivity values reach up to 215 and 1000 for CO_(g) over N_{2(g)} and decrease to 27

Table 1 Specific surface area for PCN-222, activated PCN-222 (act PCN-222), and PCN-222 grafted with corroles **2a** and **2b** (denoted as **Corr(2a)@PCN-222** and **Corr(2b)@PCN-222**). (a) and (b) Two side views of the PCN-222 MOF

	PCN-222	Act PCN-222	Corr(2a)@PCN-222	Corr(2b)@PCN-222
Specific surface area (m ² g ⁻¹)	1947.6	2143.0	1893.4	1880.1
a)				
b)				

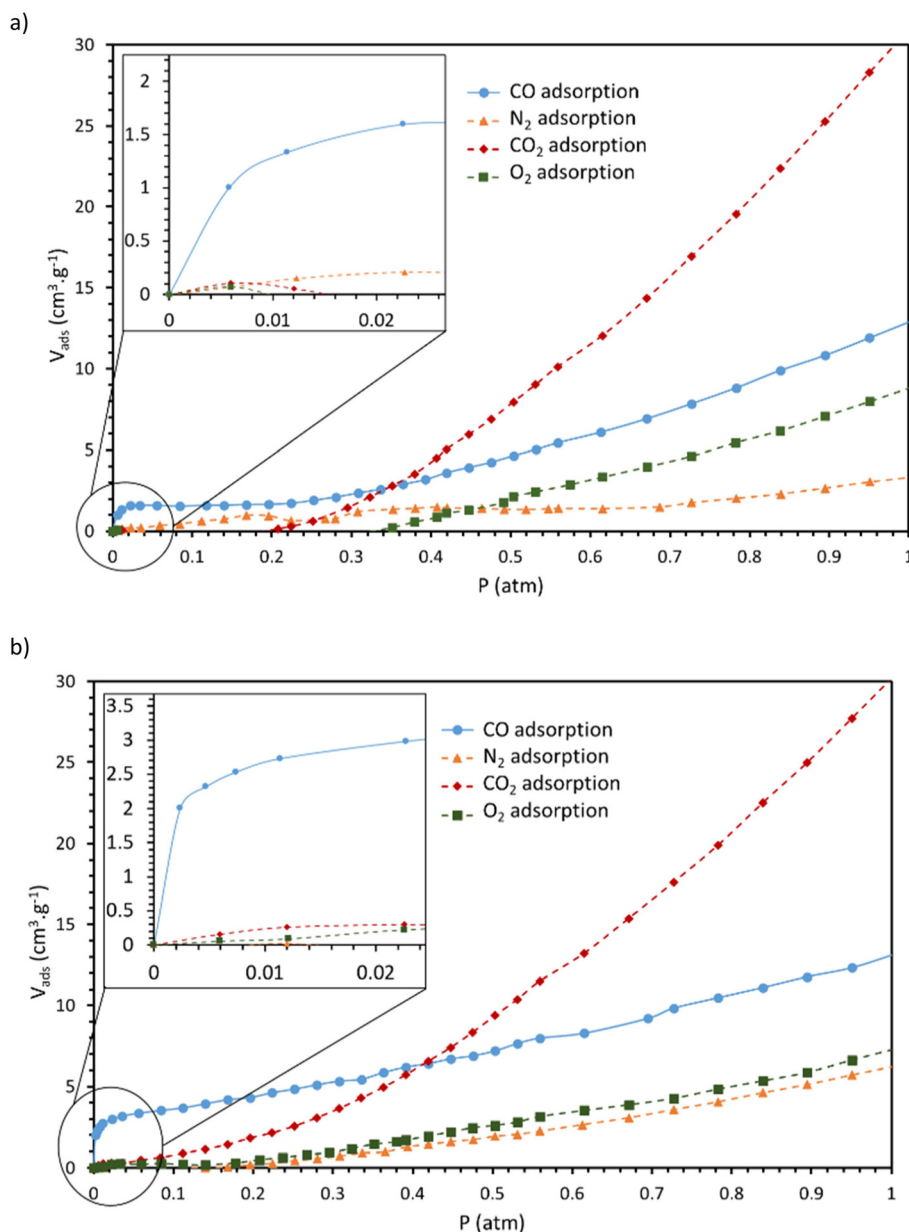


Fig. 5 Adsorption measurements of CO, CO₂, O₂ and N₂ for (a) CoCorr(2a)@PCN-222 and (b) CoCorr(2b)@PCN-222.

Table 2 Henry selectivity of PCN-222 grafted with corroles **2a** and **2b** for CO over N₂, O₂ and CO₂ at 298 K at zero loading compared with Henry selectivity of PCN-222 grafted with carboxylic acid cobalt corroles⁹ and cobalt corrole-based POPs⁸

Material	CO/N ₂	CO/O ₂	CO/CO ₂	Grafting ratio	Ref.
CoCorr(2a)@PCN-222	215	98	27	0.2	Tw=This work
CoCorr(2b)@PCN-222	1000	831	205	0.39	Tw=This work
CoCorr3@PCN-222	1776	1474	317	0.35	9
POP-CorCo-2	15 700	7380	1880	—	8

and 205 for CO_(g) over CO_{2(g)} for **CoCorr(2a)@PCN-222** and **CoCorr(2b)@PCN-222**, respectively. The best results for CO_(g) over N_{2(g)}, CO_{2(g)} and O_{2(g)} were obtained for **CoCorr(2b)@PCN-222**. In addition, if we consider the selectivity, the CO uptake at low pressure (<0.05 atm), the repeatability of the sorption measurements and the ease of the scale-up synthesis (corrole **2b** versus corrole **2a**), it turns out that **CoCorr(2b)@PCN-222** is the best candidate for functionalizing PCN-222 with a corrole for further applications in the capture or detection of CO. Compared to our previous work (Table 2), PCN-222 previously grafted with carboxylic acid corroles⁹ enables better chemisorption and selectivity than the PCN-222 grafted with phosphonic acid corroles. In order to

increase grafted material selectivity, we will need to improve the grafting ratio and the cobalt metalation of the corroles inside the MOFs.

Conclusion

In conclusion, we have developed the synthesis of A₂B-corroles bearing a phosphonic acid group at the 10-*meso*-position, which allows further linking within the cavities of the PCN-222 MOF. After cobalt metalation of the corrole macrocycle, the modified MOFs show selective CO binding with high selectivity for CO vs. CO₂, N₂, and O₂. In comparison with our previous work,⁹ carboxylic acid corroles offer slightly better chemisorption, as the CO_(g) gas uptake at low pressure was higher for carboxylic acid corroles. However, corroles functionalized with phosphonic groups offer a new and attractive alternative method for grafting porphyrinoid-type complexes into the porous structure of a MOF.

Methods

Materials and methods

See the ESI.†

Synthesis method

See the ESI.†

Characterization instruments

See the ESI.†

Author contributions

Mrs G. Divoux contributed to the synthesis and the spectroscopic characterization of the corroles. Mrs M. Loze and Dr L. André contributed to the MOF modification. The X-ray structure was solved by Dr Y. Rousselin. Writing – original draft and writing – review & editing were performed by Dr L. André, Dr N. Desbois, Dr S. Brandès and Prof. Dr Claude P. Gros. The manuscript was well discussed by all of these authors.

Data availability

The data supporting this article have been included as part of the ESI.†

Conflicts of interest

There are no conflicts to declare.

Acknowledgements

This work was supported by the Université Bourgogne Europe (UBE), the CNRS (UMR UB-CNRS 6302) and the Conseil Régional de Bourgogne through the Plan d'Actions Régional pour l'Innovation (PARI II CDEA) and the European Union through the PO FEDER-FSE Bourgogne 2014/2020. The French Research Agency (ANR) is gratefully acknowledged for financial support (ANR BioSens-Path-22-CE42-0016-02). GD thanks the ANR for a PhD grant. ML warmly thanks the Conseil Régional de Bourgogne for an ICE PhD grant. The authors thank the "Plateforme d'Analyse Chimique et de Synthèse Moléculaire de l'Université de Bourgogne" (PACSMUB, <https://www.wpcm.fr>) for access to spectroscopy instrumentation. The authors also thank Dr Quentin Bonnin and Mrs Marie-José Penouilh (Université de Bourgogne, PACSMUB) for HRMS analysis. Mrs Sandrine Pacquelet is warmly acknowledged for her synthetic contribution.

References

- 1 P. Yadav and M. Sankar, Spectroscopic and theoretical studies of anionic corroles derived from phosphoryl and carbomethoxyphenyl substituted corroles, *Chem. Phys. Lett.*, 2017, **677**, 107–113.
- 2 P. Yadav and M. Sankar, Synthesis, spectroscopic and electrochemical studies of phosphoryl and carbomethoxyphenyl substituted corroles, and their anion detection properties, *Dalton Trans.*, 2014, **43**, 14680–14688.
- 3 A. Kechiche, S. Al Shehimi, L. Khrouz, C. Monnereau, C. Bucher, S. Parola, A. Bessmertnykh-Lemeune, Y. Rousselin, A. V. Cheprakov and H. Nasri, Phosphonate-substituted porphyrins as efficient, cost-effective and reusable photocatalysts, *Dalton Trans.*, 2024, **53**, 7498–7516.
- 4 S. E. Nefedov, K. P. Birin, A. Bessmertnykh-Lemeune, Y. Y. Enakieva, A. A. Sinelshchikova, Y. G. Gorbunova, A. Y. Tsvadze, C. Stern, Y. Fang and K. M. Kadish, Coordination self-assembly through weak interactions in meso-dialkoxyphosphoryl-substituted zinc porphyrinates, *Dalton Trans.*, 2019, **48**, 5372–5383.
- 5 C. Queffelec, M. Petit, P. Janvier, D. A. Knight and B. Bujoli, Surface modification using phosphonic acids and esters, *Chem. Rev.*, 2012, **112**, 3777–3807.
- 6 Jyoti, J. An, D. Kim, D. G. Churchill and A. Kumar, Cobalt corroles: Synthesis and applications, *Coord. Chem. Rev.*, 2024, **511**, 215869.
- 7 C. Di Natale, C. P. Gros and R. Paolesse, Corroles at work: a small macrocycle for great applications, *Chem. Soc. Rev.*, 2022, **51**, 1277–1335.
- 8 S. Brandès, V. Quesneau, O. Fonquernie, N. Desbois, V. Blondeau-Patissier and C. P. Gros, Porous Organic Polymers based on Cobalt Corroles for Carbon Monoxide Binding, *Dalton Trans.*, 2019, **48**, 11651–11662.
- 9 M. Loze, S. Brandès, P. Fleurat-Lessard, N. Desbois, V. Blondeau-Patissier, C. P. Gros and L. André, CoCorrole-

- Functionalized PCN-222 for Carbon Monoxide Selective Adsorption, *Chem. – Eur. J.*, 2024, **30**, e202402148.
- 10 W. R. Osterloh, V. Quesneau, N. Desbois, S. Brandès, W. Shan, V. Blondeau-Patissier, R. Paolesse, C. P. Gros and K. M. Kadish, Synthesis and the Effect of Anions on the Spectroscopy and Electrochemistry of Mono(dimethyl sulfoxide)-Ligated Cobalt Corroles, *Inorg. Chem.*, 2020, **59**, 595–611.
- 11 M. Vanotti, S. Poisson, V. Soumann, V. Quesneau, S. Brandes, N. Desbois, J. Yang, L. Andre, C. P. Gros and V. Blondeau-Patissier, Influence of interfering gases on a carbon monoxide differential sensor based on SAW devices functionalized with cobalt and copper corroles, *Sens. Actuators, B*, 2021, **332**, 129507.
- 12 Y. Zhao, S. Hou, D. Liu and C. Zhong, Effective Adsorption of Cefradine from Wastewater with a Stable Zirconium Metal–Organic Framework, *Ind. Eng. Chem. Res.*, 2018, **57**, 15132–15137.
- 13 W. Morris, B. Voloskiy, S. Demir, F. Gandara, P. L. McGrier, H. Furukawa, D. Cascio, J. F. Stoddart and O. M. Yaghi, Synthesis, structure, and metalation of two new highly porous zirconium metal-organic frameworks, *Inorg. Chem.*, 2012, **51**, 6443–6445.